



HAL
open science

Chemical composition of microplastics floating on the surface of the Mediterranean Sea

Mikaël Kedzierski, Maialen Palazot, Lata Soccalingame, Mathilde Falcou-Préfol, Gabriel Gorsky, François Galgani, Stéphane Bruzaud, Maria Luiza Pedrotti

► **To cite this version:**

Mikaël Kedzierski, Maialen Palazot, Lata Soccalingame, Mathilde Falcou-Préfol, Gabriel Gorsky, et al.. Chemical composition of microplastics floating on the surface of the Mediterranean Sea. *Marine Pollution Bulletin*, 2022, 174, pp.113284. 10.1016/j.marpolbul.2021.113284 . hal-03955898

HAL Id: hal-03955898

<https://hal.science/hal-03955898>

Submitted on 8 Jan 2024

HAL is a multi-disciplinary open access archive for the deposit and dissemination of scientific research documents, whether they are published or not. The documents may come from teaching and research institutions in France or abroad, or from public or private research centers.

L'archive ouverte pluridisciplinaire **HAL**, est destinée au dépôt et à la diffusion de documents scientifiques de niveau recherche, publiés ou non, émanant des établissements d'enseignement et de recherche français ou étrangers, des laboratoires publics ou privés.



Distributed under a Creative Commons Attribution - NonCommercial 4.0 International License

1 **Chemical composition of microplastics floating on the surface of the Mediterranean Sea**

2 Mikaël Kedzierski*^a, Maialen Palazot^a, Lata Soccalingame^a, Mathilde Falcou-Préfol^b, Gabriel

3 Gorsky^{c,e}, François Galgani^d, Stéphane Bruzaud^a, Maria Luiza Pedrotti^c

4 ^aUniversité Bretagne Sud, UMR CNRS 6027, IRDL, F-56100 Lorient, France

5 ^bUniversity of Antwerp, Systemic Physiological and Ecotoxicological Research (SPHERE),

6 2020 Antwerp, Belgium

7 ^cSorbonne Universités, UMR CNRS 7093, LOV, F-06230 Villefranche sur mer, France

8 ^dIFREMER, LER/PAC, F-20600 Bastia, France

9 ^eResearch Federation for the study of Global Ocean Systems Ecology and Evolution,

10 FR2022/Tara Oceans-GOSEE, Paris, France

11 **Corresponding author**

12 *E-mail: mikael.kedzierski@univ-ubs.fr

13 **ABSTRACT**

14 The Mediterranean Sea is one of the most studied regions in the world in terms of microplastic
15 (MP) contamination. However, only a few studies have analyzed the chemical composition of
16 MPs at the Mediterranean Sea surface. In this context, this study aims to describe the chemical
17 composition as a function of particle size, mass and number concentrations of MPs collected in
18 the surface waters of the Mediterranean Sea. The chemical composition showed a certain
19 homogeneity at the Mediterranean Sea scale. The main polymers identified by Fourier
20 Transform Infra-Red (FTIR) spectroscopy were poly(ethylene) (67.3±2.4%), poly(propylene)
21 (20.8±2.1%) and poly(styrene) (3.0±0.9%). Nevertheless, discrepancies, confirmed by the
22 literature, were observed at a mesoscale level. Thus, in the North Tyrrhenian Sea, the proportion

23 of poly(ethylene) was significantly lower than the average value of the Mediterranean Sea
24 ($57.9\pm 10.5\%$). Anthropogenic sources, rivers, or polymer ageing are assumed to be responsible for
25 the variations observed.

26 KEYWORDS

27 Microplastics, Mediterranean Sea, FTIR, chemical composition, poly(ethylene)

28 1. Introduction

29 In recent years, plastic pollution has emerged as a major environmental and health issue (Avio
30 et al., 2017). It is defined as ubiquitous from the remote and uninhabited polar land to the
31 heights of Mount Everest (Cózar et al., 2017; Lacerda et al., 2019; Napper et al., 2020).
32 However, this pollution is mainly assessed in oceanic gyres such as subtropical regions or the
33 North Pacific gyres and in milder coastal regions such as the Mediterranean Sea (Bryant et al.,
34 2016; Cózar et al., 2015; Thiel et al., 2018). The Mediterranean Sea is a semi-enclosed sea with
35 densely populated coasts that concentrates miscellaneous intensive marine and terrestrial
36 activities and receives water from important river catchments (e.g. Nile, Ebro, Rhône and Po).
37 It is therefore no coincidence that it has been reported to be one of the largest hotspots of plastic
38 litter accumulation in the world with an estimated input of plastic of approximately 100 kt per
39 year (Cózar et al., 2015; Jambeck et al., 2015).

40 These plastic particles are composed of large proportions of microplastics (MPs) ranging from
41 millimetre-sized to micrometre-sized particles (Van Cauwenberghe et al., 2015). MPs are found
42 to be present in every studied Mediterranean shoreline and island from 18 coastal countries
43 (Fytianos et al., 2021). Despite an important spatial and temporal variability, highest
44 microplastic concentrations are found to be near the more densely populated coastlines (Pedrotti
45 et al., 2016). Statistical calculations have estimated that more than 75% of floating plastics
46 reside in the 50 km near-shore waters (Liubartseva et al., 2018). Moreover, a segregation of

47 plastic types with increasing distance to shore has been observed (Pedrotti et al., 2016). The
48 detected plastic types are diverse but some are predominant on the sea surface because of their
49 widespread use and their buoyancy: poly(ethylene) (PE), frequent in food packaging (e.g. in
50 films and bottle caps); poly(propylene) (PP), used as packaging material and plastic parts in
51 various industries; poly(amides) (PA) and poly(styrene) (PS) (Martellini et al., 2018). Polymer
52 type can be identified through different techniques. Among them, Fourier Transform Infra-Red
53 (FTIR) spectroscopy is one of the most commonly used in microplastic studies. To assess the
54 level of degradation (mainly due to oxidation by solar UV rays) by infrared spectroscopy,
55 indicators such as the carbonyl index (CI) and the hydroxyl index (HI) are generally used
56 (Julienne et al., 2019). For instance, it is well-known that the CI of PE or PP is correlated to the
57 level of degradation in air and to a lesser extent in water (Andrady, 2017, 2011; K. Zhang et al.,
58 2021). Thus, CI and the HI increase with residence time in the environment, but variability in
59 natural conditions hinder the estimation of the exposure time of MPs in the field (Chen et al.,
60 2021). However, on a larger scale, these different indices enable to compare the oxidation state,
61 and thus the degradation state of MPs collected on the sea surface.

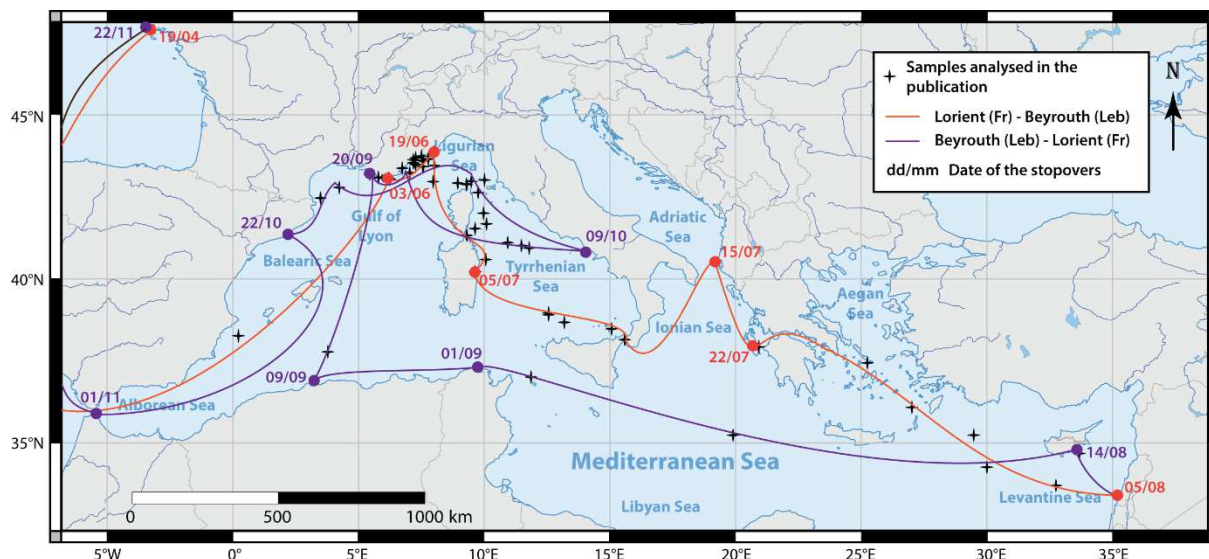
62 Despite a growing number of papers, knowledge is still lacking to fully understand the
63 distribution and concentration and chemical composition of MPs on the surface of the
64 Mediterranean Sea (Baini et al., 2018; Cincinelli et al., 2019; de Haan et al., 2019; Vianello et
65 al., 2018; Wakkaf et al., 2020; Zayen et al., 2020). A major study, carried out in 2016 on an
66 area extending from the western basin of the Mediterranean Sea to the Adriatic Sea, revealed
67 that poly(ethylene) and poly(propylene) were the most prevalent polymer categories at the sea
68 surface (Suaria et al., 2016). Furthermore, the different studies are uneasy to compare because
69 of the heterogeneity of the Mediterranean Sea environment (hydrodynamic features,
70 seasonality) and the variety of methodologies used (eg. sampling, microplastic extraction,
71 analysis, sizes considered, concentration units) (Cincinelli et al., 2019).

72 In this context, where a global vision at the scale of the Mediterranean Sea was missing, the
73 Tara Ocean Foundation, a French non-profit organisation dedicated to the study of the world's
74 oceans, carried out microplastic samplings for 5 months in 2014 across the entire Mediterranean
75 Sea. This expedition thus made it possible to map various areas using the same methodologies.
76 Therefore, this study aims to quantify and qualify microplastic pollution at the surface of the
77 Mediterranean Sea. The first section describes sample collection and preparation, the chemical
78 analysis by Attenuated Total Reflectance (ATR)-FTIR spectroscopy and the statistical
79 approach used to process the data. In the second section, the results are first described at the
80 Mediterranean Sea scale. Then results between basins are compared to evidence spatial and
81 temporal variations. In congruence with the current state of knowledge, different hypotheses
82 are proposed to explain the observed tendencies. Afterwards, methodological recommendations
83 are suggested to better investigate the microplastic pollution.

84 2. Material and methods

85 2.1. Sample collection

86 Microplastic samples were collected in Mediterranean Sea waters during the Tara Expedition
87 which was conducted between June and November 2014 (Fig. 1). Sampling was conducted
88 using a 4.4 m long manta net (mesh size: 333 μm ; net opening: 16 x 60 cm), in 154 sites which
89 were selected based on ocean colour satellite images supplied by ACRI-ST and analysed with
90 the Mercator circulation model. Geographical coordinates and dates of analysed sampling are
91 available at Zenodo Data Publisher <http://www.zenodo.org>. At each site, the manta net was
92 towed on the sea surface for ca. 60 min behind the boat at an average speed of 2.5 knots,
93 enabling thus the filtration of about 507 m^3 of seawater.



94

95 Fig. 1. Routes of the Tara Mediterranean campaign.

96 2.2. Laboratory preparations

97 2.2.1. Sample processing

98 In the laboratory, the samples were gently transferred into Petri dishes. Floating plastic debris
 99 were carefully removed from the other components (plankton, wood, etc.) to separate plastic
 100 particles, zooplankton and organic tissues. This process was done using a light box and a
 101 dissecting stereomicroscope to see the content of the samples with high contrast and ensure the
 102 removal of all the smallest and/or transparent plastic particles. Samples were double-checked
 103 to ensure the detection of all plastic particles, even the smallest ones. Blank control was
 104 removed from the analysis, including airborne textile fibres identified on the basis of their
 105 shape. The remainder of the sample was reserved for further zooplankton analysis.

106 2.2.2. Plastic analysis

107 The plastic particles were counted, measured and weighed. Firstly, plastic was digitally imaged
 108 with a ZooScan digital scanner (resolution: 2400 dpi). Then image post-processing was
 109 performed with the ZooProcess and plankton identifier software that enumerates and gives a
 110 set of morphological parameters for each object (Gorsky et al., 2010; Grosjean et al., 2004).

111 Once this step was finished, plastics samples were transferred to the Ifremer LERPAC
112 laboratory (France) to be weighed before chemical analysis. The average length (\bar{L}) of the MPs
113 per samples were calculated from the size ranges obtained by sieving. The fractions were dried
114 in an oven at 50°C for 24 hours and weighed on an electronic balance (accuracy: 0.1 mg). The
115 average mass (\bar{m}) of MPs per sample is calculated from these weighing.

116 A total of 15,654 particles, larger than 315 μm from 54 selected sites, were wet sieved by size
117 class ([5-2mm], [2-1mm], [1-0.5mm], [0.5-0.315mm]), sorted and then transferred to 96-well
118 microplates and named with a unique identifier at the Institut de Recherche Dupuy de Lôme
119 (IRD, Lorient, France) (Kedzierski et al., 2019b). The preparation was performed in an area
120 dedicated to the Tara Mediterranean Sea samples. Contamination risks were avoided during the
121 sample preparation stage by cleaning the different parts of the apparatus, especially glassware,
122 with distilled water, ethanol and/or acetone. The use of plastic apparatus was avoided as far as
123 possible. If this was impossible, spectra of these materials were obtained by Fourier Transform
124 Infrared Spectroscopy (FTIR) to check whether any potential contamination of the samples had
125 occurred.

126 2.3. Statistical approach and protocol

127 The objective here was to determine the proportions of the different chemical categories that
128 made up the particles identified via ZooScan as potentially MPs. Two cases are presented.

129 The first case consisted in determining these proportions on the scale of the entire
130 Mediterranean Sea, as well as for the three sub-basins where data were available: the Gulf of
131 Lion, the Tyrrhenian Sea and the eastern Mediterranean basin. For this purpose, 1,458
132 identifiers were randomly drawn from the database of particle identifiers (Kedzierski et al.,
133 2019b). Of these 1,458 particle identifiers, 813 were collected from the Gulf of Lion basin, 413

134 from the Tyrrhenian Sea and 227 from the eastern Mediterranean basin. The interval of
135 confidence (IC) of the proportion (p) was calculated using the following equation:

$$136 \quad IC_{\frac{\alpha}{2}} = \left[p \pm u_{1-\frac{\alpha}{2}} \sqrt{\frac{p(1-p)}{n}} \right] \quad (1)$$

137 with $u_{1-\frac{\alpha}{2}}$ the fractal of order α of the standardized normal law. As it is classical to take a
138 confidence level of 95%, then $\alpha=0.05$ and $u_{1-\frac{\alpha}{2}} = 1.96$. Finally, n is the number of particles
139 belonging to this chemical category.

140 In the second case, the proportions were studied manta by manta. In order to determine the
141 number of particles to be studied for each of the mantas, the following equation (3) was used:

$$142 \quad n = \frac{\frac{1}{4} + \frac{\varepsilon^2}{\left(u_{1-\frac{\alpha}{2}}\right)^2}}{\frac{\varepsilon^2}{\left(u_{1-\frac{\alpha}{2}}\right)^2} + \frac{1}{4N}} \quad (2)$$

143 With N the number of the manta's particles identified by the ZooScan as potentially MPs, and
144 ε the maximum value of the interval of confidence (in this study: 0.1). Once the different
145 proportions determined, the interval of confidence was refined using the following equation:

$$146 \quad IC_{\frac{\alpha}{2}} = \left[p \pm u_{1-\frac{\alpha}{2}} \sqrt{\frac{p(1-p)}{n} * \frac{(N-n)}{(N-1)}} \right] \quad (3)$$

147 The interval of confidence on the mean of results other than proportions (eg. average mass and
148 average length) was obtained from the standard deviations (σ) using the following equation:

$$149 \quad IC_{\frac{\alpha}{2}} = \left[p \pm u_{1-\frac{\alpha}{2}} \frac{\sigma}{\sqrt{n}} \right] \quad (4)$$

150 Interval of confidences for data available in the literature on the chemical nature of MPs in the
151 Mediterranean Sea were also obtained via these equations. It was thus possible to compare in
152 the discussion our results with those of the scientific literature, taking into account the varying

153 number of MPs analysed from one publication to another. Data were collected directly from
154 articles, supplementary materials, or from the authors (see “Acknowledgements”).

155 To compare the results, p-value was calculated on R using the `prop.test()` function which allows
156 for the test of Equal Proportions (Newcombe, 1998a, 1998b; The R Core Team, 2019).

157 2.4. Fourier-transform infrared spectroscopy (FTIR)

158 The MPs spectra were acquired using an Attenuated Total Reflection Fourier Transform
159 Infrared spectrometer (ATR-FTIR Vertex70v, Bruker). All spectra were recorded in absorbance
160 mode in the 4,000-600 cm^{-1} region with 4 cm^{-1} resolution and 16 scans. Each piece of plastic
161 was placed onto the germanium diamond cell (ATR Golden Gate). After each analysis of MPs
162 by ATR-FTIR, the sample holder was cleaned with ethanol. The sample chamber was also
163 cleaned out with a vacuum cleaner after every sixty analyses.

164 2.5. Determination of the chemical nature

165 FTIR spectra had already been analysed in the course of previous studies using POSEIDON
166 (Plastic pOllutionS ExtractiOn, DetectiOn and aNalysis) software which is a free and open
167 source software under development (Beta version) (Kedzierski et al., 2019b, 2019a). This
168 software, was developed with R i386 3.1.2 (The R Core Team, 2019).

169 Firstly, the software performed two pre-processing steps: first the baseline correction and then
170 the spectra normalization (Kedzierski et al., 2019a; Liland, 2015). The machine learning
171 process was performed using k-nearest neighbour classification (Ripley, 1996; Venables et al.,
172 2002). The learning database consisted in 969 spectra of MPs and other particles (natural
173 organic materials) collected during Tara 2014 scientific campaign. During the identification
174 step, if the entire k-nearest neighbour belongs to the same class, the spectrum was directly
175 identified; otherwise a majority of vote was performed. If there were less than 3 votes, the
176 spectrum was classified in the "unknown" category. In order to test the accuracy of the final

177 classification, a two steps verification was performed involving a hierarchical cluster analysis
178 and then principal component analysis (Kedzierski et al., 2019a). Then, the average spectrum
179 of each subcluster generated was calculated and verified. If the average spectrum of a subcluster
180 did not match the correct cluster, the spectrum or the group of spectra was manually identified
181 and possibly reallocated to another class. Thus, the chemical nature of 4,723 spectra was
182 analysed with POSEIDON. Results were presented for the dominant polymers (i.e.
183 poly(ethylene), poly(propylene), poly(styrene)) and the rarer categories (i.e. poly(ethylene-
184 vinyl acetate), Ethylene propylene rubber, poly(methyl methacrylate), poly(amide),
185 poly(urethane), poly(vinylchloride), poly(ethylene), and poly(propylene) like) have been
186 grouped together under the category of "Other polymers".

187 After confirmation of the plastic nature of the particles by FTIR analysis, the number of
188 microplastics and the mass of the particles could be confirmed. From these data, the
189 concentrations in number (particles/km²) and mass (mg/km²) could be calculated. From these
190 values, the average individual mass of the collected microplastics was calculated (mg).

191 2.6. Chemical indices

192 Chemical indices were calculated specifically for PE, a type of microplastic with several
193 advantages. First of all, it is ubiquitous and can be found in most samples, which allows the
194 indices to be followed over a large geographical area. Although it is possible that the
195 concentration of PE may vary over time, it can be found in all seasons. Secondly, it is often
196 present in large quantities, allowing for robust calculations. Finally, the ageing of PE samples
197 is commonly followed in the literature with these indices in both artificial and natural
198 conditions.

199 To evaluate the state of ageing of PE, two indices, the carbonyl index (CI) and the hydroxyl
200 index (HI) were modified after Julienne et al., 2019:

201 $CI = \frac{I_{1800-1700}}{I_{1480-1460}}$ (5)

202 $HI = \frac{I_{3900-3200}}{I_{1480-1460}}$ (6)

203 A new index, called fouling index (FI), was also developed as part of this study to account for
204 the extra band appearing on many PE spectra between 1,040 and 1,020 cm^{-1} (Kedzierski et al.,
205 2019b, 2019a):

206 $FI = \frac{I_{1040-1020}}{I_{1480-1460}}$ (7)

207 2.7. Other variables

208 From the total number of microplastics collected (N) and the percentage of PE (PE_p), the
209 number of PE particles (N_{PE}) was calculated for each of the 54 samples studied. Then, the
210 number of PE spectra to be analyzed (n_{PE}) was determined by randomly drawing 10% of the
211 N_{PE} for each of the 54 manta samples. Thus, a total of 1,086 PE spectra were randomly selected
212 for the calculation of the indices. This process was carried out 100 times in order to limit
213 variability: the average indices were obtained from these 100 calculation processes. All the
214 calculations were carried out with the R software i386 3.1.2 (The R Core Team, 2019). The
215 results obtained were then compared with the help of a z-test thanks to the `z.test()` function
216 available in the BSDA library of R.

217 2.8. Presentation of the results

218 All the results were expressed at several spatial scales: at the Mediterranean Sea scale, at the
219 scale of the main sub-basins of the Mediterranean Sea (i.e. Gulf of Lyon, Tyrrhenian Sea, and
220 Eastern Basin), and at the scale of the sampling area. An intermediate scale was also introduced
221 to facilitate the link between the sub-basin and the sampling area scales. It groups the results
222 obtained every 2° of latitude (eg. between 36 and 38°E), and every 10° of longitude (eg.

223 between 0 and 10°E). Similarly, over time, the results were also presented by month. Grouping
224 the results in this way reduces the uncertainty associated, and facilitate the identification of
225 anomalies through statistical tests.

226 3. Results

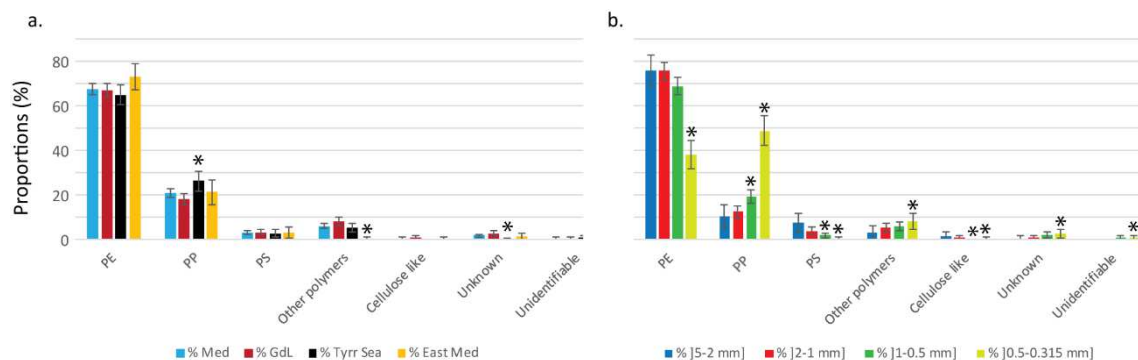
227 3.1. Overview of the microplastic pollution in the Mediterranean sea and its sub-basins

228 3.1.1. Chemical composition and indices

229 The collected particles were mainly PE ($67.3\pm 2.4\%$), PP ($20.8\pm 2.1\%$), and PS ($3.0\pm 0.9\%$) (Fig.
230 2.a). The other identified polymers (i.e. poly(ethylene-vinyl acetate), ethylene propylene
231 rubber, poly(methyl methacrylate), poly(amide), poly(styrene), poly(urethane),
232 poly(vinylchloride), and poly(ethylene) and poly(propylene) like) represented $6.0\pm 1.2\%$ of the
233 total sampled particles. Thus, MPs represented about 97% of the particles identified as such by
234 the ZooScan. For the three sub-basins studied (Gulf of Lyon, Tyrrhenian Sea and eastern
235 Mediterranean basin) the distribution of polymer types was similar to the one observed at the
236 Mediterranean Sea scale. Nevertheless, in the Tyrrhenian Sea, the PP rate was significantly
237 higher than the average value of the Mediterranean Sea. In the Eastern Mediterranean basin,
238 the data showed a significantly lower rate of the category “other polymers”. The proportions of
239 the different chemical natures highlighted in this study varied significantly according to the
240 particle size range (Fig. 2.b). Thus, the PE content of the samples was $76.1\pm 7.0\%$ for particles
241 between 2 and 5 mm, and fell to only $38.3\pm 6.4\%$ in the 315 to 500 μm particle size range. PS
242 showed a similar tendency, with proportions of $7.7\pm 4.4\%$ to $0.5\pm 0.9\%$ respectively.
243 Conversely, the PP content of the samples increased as the particle size range decreased. Indeed,
244 PP represented 10.6% of the particles for particles between 2 and 5 mm, and increased up to
245 $49.1\pm 6.6\%$ in the particle size range from 315 to 500 μm . Thus, the PP/PE ratio remained
246 relatively constant for MP belonging to the size classes between 500 μm and 5 mm with values

247 in the range of 0.2 to 0.32. It then increased sharply to a value of 1.5 for particles in the 315 μm
248 to 500 μm size range.

249 For the other chemical natures, no significant variation was observed. Regarding the indices,
250 the mean values were 0.77 ± 0.02 for the Carbonyl Index (CI), 2.88 ± 0.16 for the Hydroxyl Index
251 (HI) and 0.45 ± 0.02 Fouling Index (FI).



252
253 Fig. 2. Proportion of the chemical natures of the MPs collected (\pm Interval of confidence). a.
254 Proportions of the different chemical natures at the Mediterranean scale (Med) as well as for
255 the three sub-basins studied: the Gulf of Lyon (GdL), the Tyrrhenian Sea (Tyrr Sea) and the
256 eastern Mediterranean basin (East Med) (\pm Interval of confidence). The chemical composition
257 varied little from one basin to another. Only the Tyrrhenian Sea had a significantly (*) higher
258 PP content than the Mediterranean Sea. b. Proportions of the different chemical natures
259 according to the size range of the collected particles (\pm Interval of confidence). Statistically
260 significant variations (*) of the chemical nature were evidenced depending on the size range
261 studied.

262 3.2. Spatial and temporal variations

263 3.2.1. Chemical nature

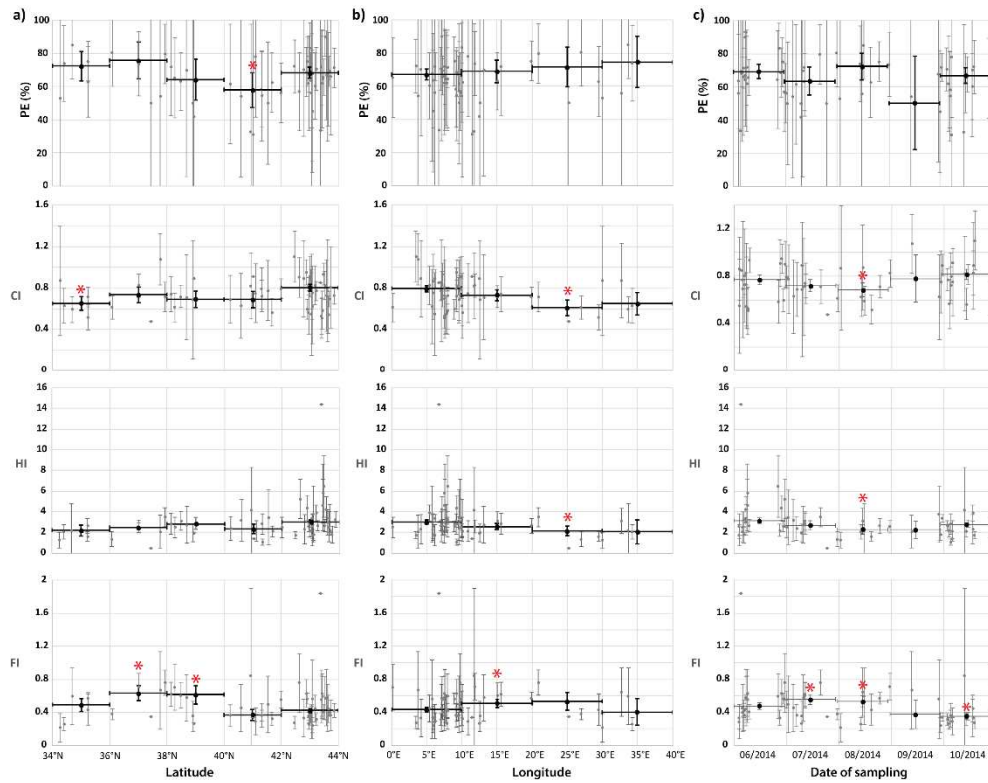
264 The PE proportions changed little with latitude and remained close to the Mediterranean Sea
265 average (Fig. 3.a). However, it was significantly lower between 40 and 42°N latitude (i.e.

266 57.9±10.5%), corresponding to samples from the northern Tyrrhenian Sea. The CI was
267 significantly lower between 34 and 36°N (i.e. 0.65±0.07), matching samplings from the eastern
268 Mediterranean Sea basin. For the other latitudes, no significant difference from the
269 Mediterranean average could be found. The HI also showed little variation and none that was
270 statistically significant. Lastly, the fouling index was characterized by larger variations, and
271 significantly larger values between 36 and 40°N (i.e. 0.63±0.09 and 0.61±0.11). Finally, these
272 four variables all showed the same general pattern suggesting an increase that was more or less
273 marked from 34 to 38°N latitude, then a decrease from 38 to 42°N latitude and finally an
274 increase from 42 to 44°N latitude.

275 Although not significant compared to the average of the Mediterranean Sea, the percentage of
276 PE in the samples tended to increase with increasing longitude (Fig. 3.b). However, the
277 variability also tended to increase at the same time. Thus, this trend did not result into
278 statistically significant variations. The CI tended to decrease between 0 and 30°E longitude and
279 was significantly lower (i.e. 0.61±0.08) between 20 and 30°E. A similar pattern was identifiable
280 for the HI, with a significantly lower mean value between 20 and 30°E longitude (i.e. 2.1±0.48).
281 Finally, in the case of the FI, a different trend was observed with an increase between 0 and
282 30°E longitude, with a significantly different value between 10 and 20°E longitude (i.e.
283 0.51±0.05). Then, between 20 and 40°E longitude, the FI decreased.

284 Over the sampling period, the monthly averages did not differ significantly in terms of
285 percentage of PE. The CI was characterized by variations whose general pattern suggested a
286 seasonal signal. Indeed, the CI decreased from June to August, reaching for this last month a
287 significantly lower value (i.e. 0.68±0.06). Then from August to October, the CI values increased
288 again. The same pattern was visible for the HI with a decrease from June to August and an
289 increase from August to October. For this index the mean value in August was significantly
290 lower with 2.29±0.45. On the contrary, the FI study showed an inverse tendency with an

291 increase from June to August and a decrease from August to October: the FI value of July and
 292 August were significantly higher (0.56 ± 0.06 and 0.53 ± 0.07 , respectively), while that of October
 293 was significantly lower (0.36 ± 0.01).



294

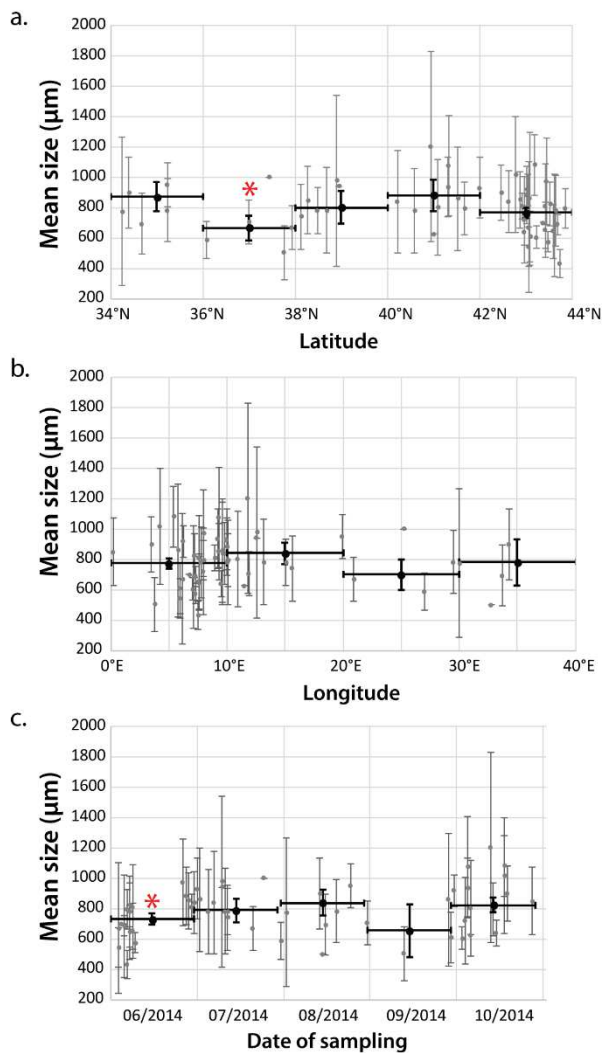
295 Fig. 3. Evolution of the percentage of PE and the associated indices (CI: carbonyl index; HI:
 296 Hydroxyl index; FI: Fouling index) as a function of latitude, longitude and sampling period
 297 (\pm Interval of confidence). a. Evolution of the four variables as a function of latitude. b.
 298 Evolution of the four variables as a function of longitude. c. Evolution of the four variables as
 299 a function of the sampling date.

300 3.2.2. Particle size

301 The mean size of the collected microplastics was stable according to the latitude of collection,
 302 except between 36 and 38°N with a mean value of 667 ± 80 μm . This value was significantly
 303 lower than the mean value of the Mediterranean Sea (Fig. 4.a). In contrast, between 34-36°N,
 304 38-40°N, 40°-42°N, and 42°-44°N the mean sizes were respectively $871\pm 98\mu\text{m}$, 800 ± 109 μm ,

305 883±104 μm, 765±31 μm, which were not significantly different from the Mediterranean Sea
306 mean value.

307 In terms of longitude, the mean was stable and no significant variation could be found for the
308 longitude ranges between 0-10°E (772±31 μm), 10-20°E (840±68 μm), 20-30°E (700±100 μm),
309 30-40°E (780±150 μm) (Fig. 4.b). Concerning the sampling date, June samplings showed a
310 significantly smaller mean size (730±39 μm) whereas no significant variation in mean size
311 could be demonstrated for the following months (July: 789±76 μm; August: 837±85 μm;
312 September: 654±176 μm; October: 823±50 μm) (Fig. 4.c).

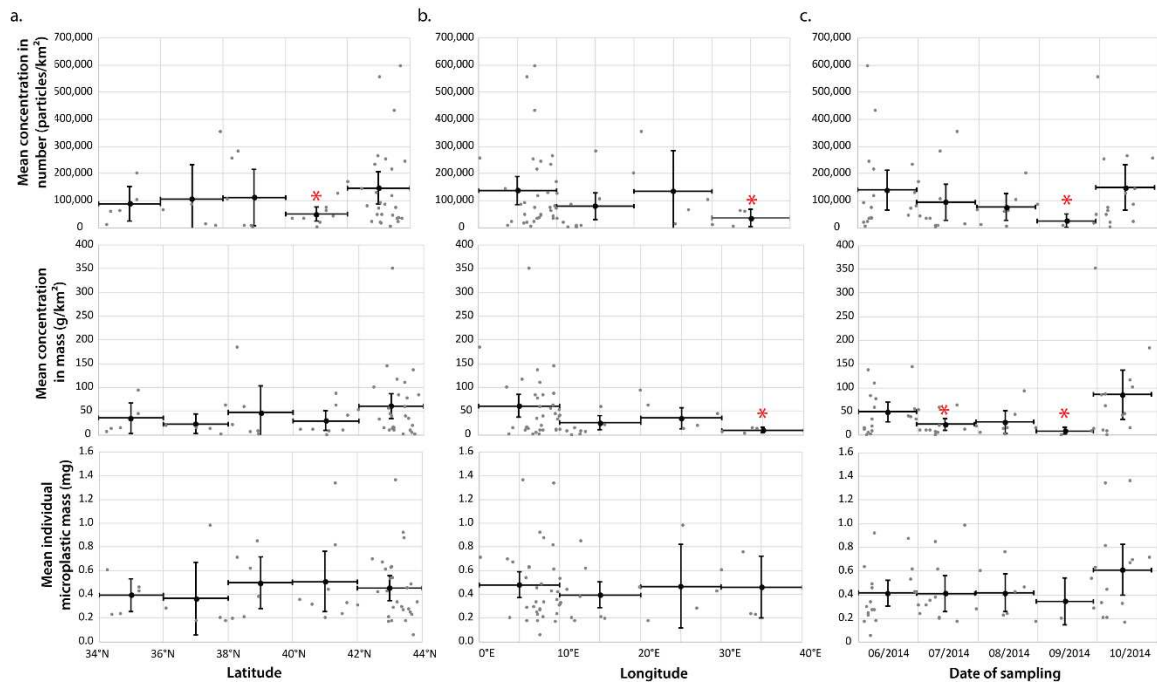


313

314 Fig. 4. Evolution of the microplastic mean size as a function of latitude (a.), longitude (b.) and
315 sampling date (c.) (\pm Interval of confidence). The mean size was globally homogeneous and
316 little statistically significant change (*) could be demonstrated through space and time.

317 3.2.3. Concentrations

318 The mean concentration in number was stable for the different latitude ranges and the only
319 significantly lower value (i.e. $50,438 \pm 25,130$ particles/km²) was between 40 and 42°N latitude
320 (Fig. 5.a). The study of these variables as a function of longitude did not reveal a clear trend
321 (Fig. 5.b). Thus, the mean concentration in number showed little variation except between 30
322 and 40°E, which was significantly lower (i.e. 35.278 ± 31.433 particles/km²). Similarly, for the
323 mean concentration in mass, the only significantly different value was between 30 and 40°E,
324 with a mean value of 10.0 ± 5.4 g/km². Finally, in the case of the mean concentration in number
325 and in mass as a function of the sampling periods, the variations could suggest a seasonal signal
326 (Fig. 5.c). Thus, the mean concentration in number decreased from June to September, with a
327 significantly lower mean value in September (i.e. $25,800 \pm 24,300$ particles/km²). Then, in
328 October, the mean value increased. A similar pattern could be described for the mean contraction
329 in mass with a decrease from June to September and an increase in October. Two mean values
330 appeared significantly lower, those of July (23.3 ± 12.5 g/km²) and especially September
331 (8.8 ± 7.3 g/km²).



332

333 Fig. 5. Evolution of the mean concentrations in number and in mass, and mean individual
 334 microplastic mass as a function of latitude (a.), longitude (b.) and sampling date (c.) (\pm Interval
 335 of confidence).

336 3.2.4. Seasonality

337 In order to test the hypothesis of a seasonal fluctuation of the variables, it was possible to rely
 338 on the comparison of samples taken at different periods in the same geographical area (Tab. 1).
 339 For this purpose, the results obtained in the areas of the Gulf of Lyon in June and September-
 340 October, as well as in the Tyrrhenian Sea in June-July and October were compared. This
 341 comparison for these two areas did not reveal any significant difference between the sampling
 342 periods for most values (e.g. mean size, concentration in number, percentage of PE, CI). In
 343 contrast, the concentration in mass and the mean individual showed larger discrepancies.
 344 However, the large variability in sample mass did not allow to highlight a statistically
 345 significant difference. The only significant differences were observed for HI (Tyrrhenian Sea)
 346 and FI (Tyrrhenian Sea, Gulf of Lyon).

347 Table. 1. Results of the different sampling periods in the Gulf of Lyon and the Tyrrhenian Sea
 348 (\pm Interval of confidence; *: significant value).

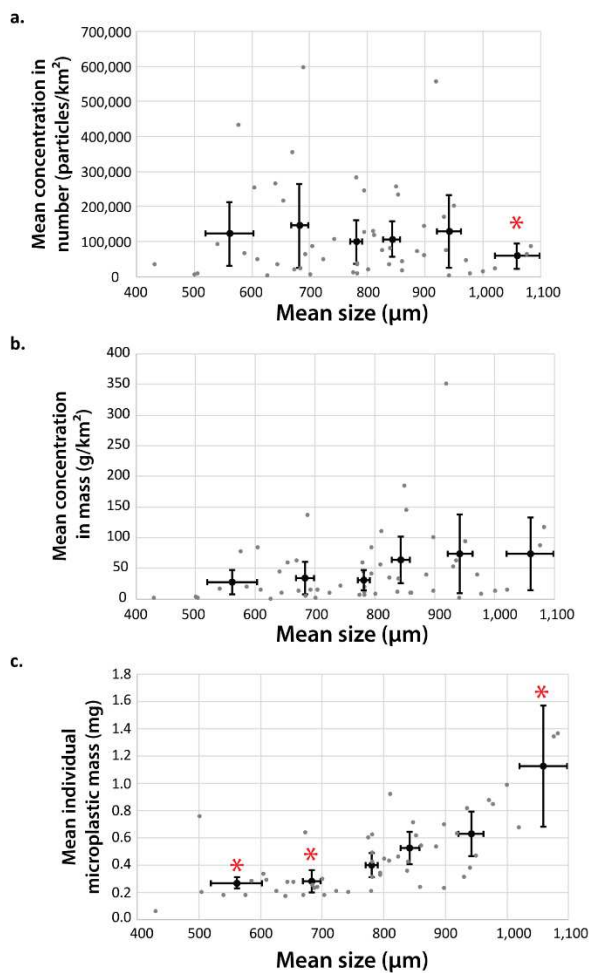
	Gulf of Lyon		Tyrrhenian Sea	
	Jun.	Sept.-Oct	Jun.-Jul.	Oct.
Date of sampling	Jun.	Sept.-Oct	Jun.-Jul.	Oct.
Number of sampling	14	8	13	7
Mean size (μm)	698 \pm 14	839 \pm 23	847 \pm 10	867 \pm 52
Concentration in number (particles/ km^2)	141,878 \pm 92,512	148,167 \pm 126,955	93,651 \pm 48,624	82,051 \pm 73,477
Concentration in mass (g/km^2)	43.7 \pm 22.9	88.4 \pm 80.1	35.3 \pm 21.1	57.8 \pm 42.7
Average individual microplastic mass (mg)	0.4 \pm 0.1	0.6 \pm 0.3	0.4 \pm 0.1	1.8 \pm 2.7
PE (%)	69.3 \pm 4.9	69.1 \pm 5.9	66.5 \pm 6.5	63.6 \pm 11.5
CI	0.8 \pm 0.02	0.9 \pm 0.02	0.8 \pm 0.02	0.8 \pm 0.03
HI	3.0 \pm 0.34	2.9 \pm 0.1	3.2 \pm 0.12*	2.5 \pm 0.22*
FI	0.4 \pm 0.04*	0.3 \pm 0.01*	0.4 \pm 0.02*	0.4 \pm 0.04*

349

350 3.3. Potential interactions between variables and particle size

351 3.3.1. Concentration

352 The manta by manta study of the mean concentration in number (Fig. 6.a) and in mass (Fig.
 353 6.b) as a function of the microplastic mean size did not reveal any significant variation except
 354 above 1,000 μm with a marked lower value of $58,043 \pm 36,010$ particles/ km^2 . On the other hand,
 355 quite logically, the mean individual microplastic mass increased strongly when the mean size
 356 increased (Fig. 6.c). Thus, the extreme values were significantly different from the average
 357 mass value calculated at the Mediterranean Sea scale. At the Mediterranean scale, an average
 358 density of microplastics of about 0.9 could be calculated from these data. This value is
 359 consistent with that of PE and PP particles (Kedzierski et al., 2017).

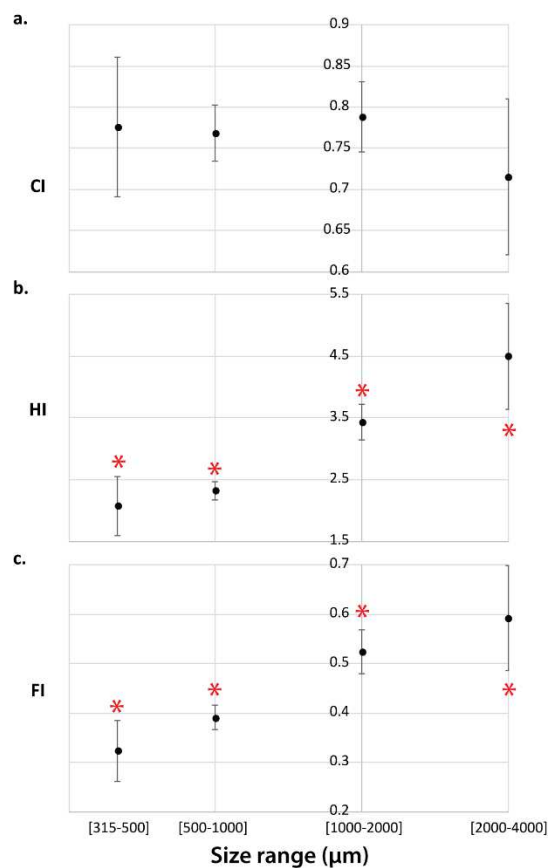


360
 361 Fig. 6. Evolution of the concentrations in number and in mass, and average individual mass
 362 (\pm Interval of confidence) as a function of average size of the microplastics (\pm Interval of
 363 confidence). a. Evolution of the concentrations in number as a function of average size of the

364 microplastics. Few significant differences can be identified (*). b. Evolution of the
365 concentrations in mass as a function of average size of the microplastics. No statistical
366 difference could be demonstrated. c. Evolution of the average individual mass as a function of
367 average size of the microplastics. A clear increase of the mass of microplastics when the size
368 of these increases was highlighted.

369 3.3.2. PE indices

370 The different indices calculated from the PE spectra showed different size-dependent
371 evolutions. The CI (Fig. 7.a) did not show significant variation with size in contrast to the HI
372 (Fig. 7.b) and FI (Fig. 7.c) which both showed clearly an increase as the microplastic size class
373 increased. Thus, HI and FI increased from 2.1 ± 0.5 and 0.32 ± 0.06 for the [315-500] μm size
374 range to 4.5 ± 0.9 and 0.59 ± 0.11 for the [2,000-5,000] μm size range respectively. The values
375 obtained were statistically different from the average values calculated at the Mediterranean
376 Sea scale (HI: 2.88 ± 0.02 and FI: 0.45 ± 0.02).



377

378 Fig. 7. Evolution of the CI (a.), the HI (b.) and the FI (c.) indices calculated from the PE spectra
 379 as a function of the size range (\pm Interval of confidence). No significant variations of CI (*) were
 380 found. The HI and FI, show a particular pattern where each size class is significantly different
 381 (*) from the Mediterranean mean values.

382 4. Discussion

383 4.1. Chemical composition of MPs on the surface of the Mediterranean Sea

384 4.1.1. Comparison with previous work and limitations

385 Few studies have analysed more than a few hundred MPs in the Mediterranean. Among them,
 386 Baini et al. (Tuscany, Italy) and Zeri et al. (Adriatic Sea) have shown chemical composition
 387 results very similar to those of our study (Baini et al., 2018; Zeri et al., 2018): PE rates of about
 388 $66.0 \pm 5.2\%$ and $66.5 \pm 2.6\%$ respectively. On the contrary, other studies have shown different
 389 results, with notably lower PE rates: $41.2 \pm 3.3\%$ in the south of the Adriatic Sea (Suaria et al.,

390 2016), $60.0\pm 1.9\%$ in the north of this sub-basin (Vianello et al., 2018), $55.0\pm 1.7\%$ and
391 $43.0\pm 4.6\%$ in the western basin of the Mediterranean Sea (de Haan et al., 2019; Suaria et al.,
392 2016). The results of these two publications differ significantly from those of our publication.
393 In contrast, two other studies have evidenced high percentages of PE in the range of 76 ± 3.9 to
394 $79\pm 5.4\%$ on the southern coasts of the Mediterranean Sea. Nevertheless, these values are
395 consistent with those found by the present study ($73.1\pm 5.8\%$) in the eastern Mediterranean Sea
396 basin. Finally, it is interesting to note that the PE rate in the Mediterranean Sea is on average
397 higher than in the Atlantic ocean ($<60\%$) (Enders et al., 2015).

398 However, the comparison of the data obtained between our study and these publications
399 presents various limitations (Baini et al., 2018; de Haan et al., 2019; Suaria et al., 2016; Vianello
400 et al., 2018; Zeri et al., 2018). The first is undoubtedly linked to a scale effect. Indeed, the
401 smaller the sampling in terms of number of sampling points, the more sensitive it will be to
402 local variations. Thus, it may be more prone to deviate from the average value for the
403 Mediterranean Sea. However, the lack of data leads to the comparison of studies carried out at
404 different spatial scales, which necessarily raise the question of the relevance of the differences
405 highlighted. The use of statistical calculations considering the number of particles analysed (i.e.
406 calculation of the interval of confidence, proportion test) allows to partially compensate this
407 bias of geographical scale.

408 Furthermore, the lack of standardised sampling methods is a hindrance when it comes to
409 comparing MPs studies with each other (Cincinelli et al., 2019). The influence of the net mesh
410 size is assumed to be crucial in MPs size measured. For example, sampling in the Seine River
411 with an $80\mu\text{m}$ net yields on average 30 times more MPs (in numbers) than sampling with a
412 $333\mu\text{m}$ net (Gasperi et al., 2014). As it can differ between publications, discrepancies in MP
413 concentrations, but also in PE proportions, could be induced by this parameter. Moreover, as

414 observed in the present study and in previous ones, the PP proportions tends to increase with
415 decreasing size range in the Mediterranean Sea (Baini et al., 2018). Thus, the polymer
416 proportions measured could be partially dependent on the sampling methods.

417 4.1.2. 4.1.2. PP/PE ratio and the size range

418 First of all, the evolution of the PP/PE ratio according to the size range of the MPs should be
419 discussed. An increase in the PP rate with decreasing particle size has been demonstrated in the
420 Mediterranean Sea by Baini et al. (Baini et al., 2018). This tendency was observed to be steadier
421 and stronger than in our study but in both cases the general pattern remains the same. The same
422 pattern was also found on plastic samples from different oceans and could be related according
423 to the authors to different degradation behaviours of PP and PE in sea water (Serranti et al.,
424 2018). In fact, this trend could be explained by a higher ageing sensitivity of PP than PE,
425 enabling PP to fragment into small dimensions faster (Gewert et al., 2015). This ratio therefore
426 seems to be an interesting data to characterise plastic pollution, and may be an indicator of a
427 segregation phenomenon undergone by plastic pollution on the ocean surface.

428 4.1.3. PE indices

429 Although indices are widely used to characterise the state of atmospheric weathering of PE,
430 they should be taken with greater caution when working on PE aged in the marine environment.
431 In the present results, the CI was homogeneous at the Mediterranean Sea scale. The weathering
432 state of polymers is assumed to be homogeneous at the surface of the Mediterranean Sea: highly
433 degraded PE (i.e. with high CI values) tending either to fragment into particles smaller than
434 300µm or to sediment. It is also quite possible that in the marine environment a threshold value
435 exists for CI (Andrady, 2017).

436 For HI and FI, it is likely that the observed seasonal variations may be related to variations in
 437 the plastisphere. At this stage, it is difficult to interpret these temporal variations from a
 438 biological point of view. However, as the spectrometric approach is now relatively common for
 439 the chemical analysis of microplastics, the acquisition of plastisphere spectra would be
 440 relevant. The decrease in FI and HI with decreasing PE microparticle size, can be interpreted
 441 as a sign of a more limited implantation of the plastisphere on the surface of small microplastics.
 442 This phenomenon could be explained by a greater susceptibility of small microplastics to
 443 sedimentation.

444 4.2. Variations observed at smaller geographical scale

445 4.2.1. A truly heterogeneous sea?

446 Despite these methodological differences, could the differences observed between publications
 447 be explained by a heterogeneous chemical nature of MPs floating on the surface of the
 448 Mediterranean Sea? If our study tends to highlight differences in polyethylene levels, the
 449 analysis of previous scientific publications also seems to show some similar trends.

450 In the end, the average chemical compositions observed in the Mediterranean Sea can be
 451 summarised in four main patterns (P1-4) illustrating the small heterogeneities occurring in this
 452 basin (Tab. 2).

453 Tab. 2. Proposal of four main patterns to describe the state of contamination of the
 454 Mediterranean Sea by MPs.

Pattern	Area	Proportions (this study and other publications)	Example other than the current study

P1	North Tyrrhenian Sea	PE: $\leq 65\%$ PP: $> 25\%$ Others: 5-15%	(Baini et al., 2018)
P2	North of the Mediterranean Sea	PE: 65-70% PP: 15-20% Others: 5-15%	(Vianello et al., 2018)
P3	South of the Mediterranean Sea	PE: $> 70\%$ PP: 15-25% Others: $< 10\%$	(Wakkaf et al., 2020; Zayen et al., 2020)
P4	P4: Centre of the western basin / maritime traffic convergence areas	PE: $< 60\%$ PP: 5-25% Others: $> 20\%$	(de Haan et al., 2019; Suaria et al., 2016)

455

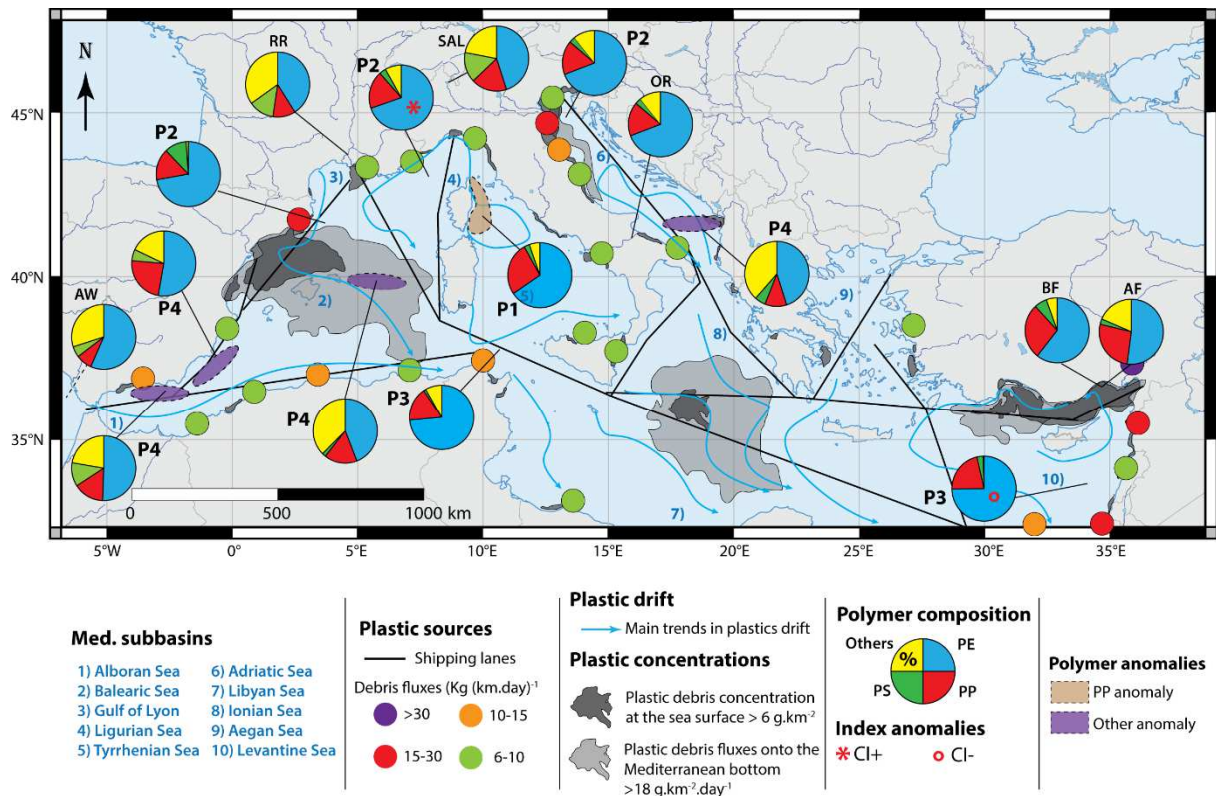
456 Based on this reflection, it is possible to question this heterogeneity and its origin. To this end,
457 some hypotheses can be proposed to explain these differences. Some of them are presented
458 through three cases: the North Tyrrhenian Sea, the South Mediterranean Sea and the case of the
459 pattern 4.

460 4.2.2. The case of the North Tyrrhenian Sea

461 In the Northern Tyrrhenian Sea, the PE and PP proportions were respectively abnormally low
462 and high (P1; Fig. 8) compared to other sampled areas in the Northern Mediterranean Sea (P2;
463 Fig. 8). This lower proportions of PE in the North Tyrrhenian Sea could imply the existence of
464 local sources introducing MP pollution with low levels of PE (i.e. $< 65\%$ of PE). These MPs can
465 come from four main sources: rivers, cities, maritime traffic and sea currents (Liubartseva et

466 al., 2018; Soto-Navarro et al., 2020) (Fig. 8). There are currently no data for the Italian rivers
467 flowing into the Tyrrhenian Sea. Based on data further away from this geographical framework,
468 it appears that the composition of MP pollution in European rivers is generally poor in PE and
469 rich in PP and PS. Indeed, PE proportions have been reported to be quite low in samples
470 collected on the surface of lakes tributary of the Po (SAL; Fig. 8) and in the delta of the Rhône
471 river (RR; Fig. 8) with levels of about 40% to 45% respectively (Constant et al., 2020; Imhof
472 et al., 2013; Sighicelli et al., 2018). Other publications on north European rivers (without
473 connection to the Mediterranean Sea) also have highlighted relatively low percentages of PE
474 (<50%) (Mani et al., 2015). Furthermore, the relatively high average size and mass of the MPs
475 collected in the north of the Tyrrhenian Sea can possibly be interpreted as an indication of a
476 source of microplastic relatively close to the sampling areas.

477 Cities such as Rome, Naples or Livorno are other potential important sources of MPs
478 (Liubartseva et al., 2018; Soto-Navarro et al., 2020). However, data are very scarce in the case
479 of Mediterranean cities and, more generally, in the case of this kind of proximal sources that
480 therefore need to be better studied (de Haan et al., 2019). In other locations around the world,
481 MPs observed in cities (i.e. water and soils) are heterogeneous and have rather low PE contents
482 (Wu et al., 2020; Yan et al., 2019; L. Zhang et al., 2021).



483

484 Fig. 8. Synthesis map of the sources, drift, concentration and composition of MPs in the
 485 Mediterranean Sea. Data on sources, concentrations and drifts of MPs are based on numerical
 486 modelling (Liubartseva et al., 2018). The data on chemical types are taken from the current
 487 study and various other publications (listed hereafter). Patterns – P1 to P4 (Baini et al., 2018;
 488 de Haan et al., 2019; Suaria et al., 2016; Vianello et al., 2018; Wakkaf et al., 2020; Zayen et al.,
 489 2020). Atlantic – AW: Atlantic waters (Enders et al., 2015). Rivers – RR: Rhône river (Constant
 490 et al., 2020); OR: Ofanto river (Campanale et al., 2020); SAL: Subalpine lakes (Sighicelli et
 491 al., 2018). Flooding – BF: Before flooding; AF: After flooding (Gündoğdu et al., 2018).

492 4.2.3. The case of the Levantine Sea

493 Although not significant, the PE proportions observed in our study are on average higher in the
 494 Levantine Sea region than in the rest of the Mediterranean. Statistically different from the
 495 average value for the Mediterranean Sea, two other studies have evidenced high percentages of
 496 poly(ethylene) (P3; Fig. 8), supporting the idea that the PE proportions seems higher in the

497 South than in the North of the Mediterranean (Wakkaf et al., 2020; Zayen et al., 2020). Although
498 the literature on MPs and its chemical nature is excessively limited regarding major rivers of
499 the Mediterranean Sea, this North-South difference could be explained by the rivers. This is
500 particularly true for the Nile, since only one study has been conducted to date. This lack of
501 knowledge has been identified as a major handicap in understanding the plastic pollution in the
502 Mediterranean Sea (Guerranti et al., 2020; Khan et al., 2020; Martellini et al., 2018). Yet,
503 according to modelling studies, the Nile is supposed to be one of the major MP contributor and
504 to strongly influence the chemical nature of MPs in the Mediterranean Sea (Lebreton et al.,
505 2012; Liubartseva et al., 2018; Soto-Navarro et al., 2020). By widening the geographical
506 framework, it is possible to note that high PE percentages of around of 76.9% have been
507 reported for the Ofanto river (OR, Fig. 8) in southern Italy (Campanale et al., 2020). In addition,
508 a recent study carried out on the surface of the Bizerte lagoon (Tunisia) has shown very high
509 percentages of PE (79%) (Wakkaf et al., 2020). Thus, unlike the Tyrrhenian Sea, it is possible
510 that the southern rivers of the Mediterranean Sea tend to contribute to high percentages of PE
511 resulting in local anomalies. Furthermore, even though no seasonal variation was detected in
512 the southern Mediterranean Sea during our sampling campaign, PE proportions have been
513 reported to be high during periods of lower river flows (BF; Fig. 8) whereas they tend to
514 decrease during intense rainfalls (AF; Fig. 8) (Gündoğdu et al., 2018). The same trend was
515 observed in southern India where marked seasonality exists (Veerasingam et al., 2016). This
516 alternating water regime is observed throughout the southern Mediterranean Sea (Djellouli-
517 Tabet, 2010; Varis et al., 2019), implying that the Levantine Sea would be fed by rivers with
518 high PE levels during the summer period. If this hypothesis is correct, then there should be a
519 stronger seasonal signal in the southern Mediterranean Sea. Thus, the difference between the
520 north and the south should be more pronounced in summer than in winter. As the Tyrrhenian
521 Sea and the Gulf of Lyon, all located in the northern part of the Mediterranean Sea, have shown

522 a possible seasonality, the sampling campaign may have missed a seasonality phenomenon in
523 its southern part.

524 4.2.4. Pattern 4 (P4)

525 The P4 pattern was not found in our results, but appears in some regions such as the central
526 western basin (Fig. 8) (Suaria et al., 2016). Driven by winds and sea currents, MPs from the
527 Gulf of Lyon and the Balearic Sea then travel about 900 km to arrive off the Maghreb coasts
528 (Liubartseva et al., 2016). Two main sources probably supply the centre of the western basin in
529 MPs: plastic pollution present in the north of the basin on the one hand and the maritime traffic
530 on the other hand. As they move away from land-based sources, it is likely that microplastics
531 tend to settle to the ocean floor or fragment below 300µm. Then, microplastic pollution
532 probably tends to become more sensitive to plastic inputs from marine sources. Marine sources
533 consist, among other things, of inputs of very dense polymers such as boat paint (Suaria et al.,
534 2016). Thus, high levels of dense polymers (22%) were observed in this area (Suaria et al.,
535 2016). It is therefore quite possible that the very important maritime traffics in this region of
536 the Mediterranean, combined with a low contribution via land sources, could be the origin of
537 P4 (Fig. 8).

538 It is also possible that the importance of maritime traffic can also explain the presence of the
539 P4 in the southern Adriatic Sea (PA, paint) and in the Alboran Sea (polyacrylic ship paint) (de
540 Haan et al., 2019; Suaria et al., 2016).

541 4.3. Methodological contributions and recommendations

542 Some methodological aspects are discussed to temper the results observed in the present study.
543 First, sampling in the same area at different dates was a relevant strategy to discriminate
544 between variations of seasonal origin and those of spatial origin. For example, this strategy has

545 shown that the difference between the northern Tyrrhenian Sea and the rest of the
546 Mediterranean Sea was not seasonal, but geographical. Nevertheless, in the southern basin,
547 some doubts still exist about a potential seasonal phenomenon. Thus, in future work, conducting
548 periodic samplings in the southern region would fill the blanks in seasonality assumptions.

549 Second, another approach that proved useful for this work was to seek to have a large number
550 of sampling points, and to analyse only a fraction of the microplastics collected. This strategy
551 kept the analysis effort at an acceptable level while obtaining more global results, less sensitive
552 to the significant variability of the sampling points. Coupled with statistical tests, this approach
553 made it possible to easily identify, for each of the parameters studied, the significantly different
554 areas.

555 Spatially homogeneous sampling is also desirable. In the context of this study, the smaller
556 number of sampling points in the eastern basin, mainly due to the geopolitical context of the
557 south-east Mediterranean Sea at the time of the sampling campaign, implied a greater
558 uncertainty in the results. It would therefore be desirable in the future to increase the research
559 effort in the eastern Mediterranean Sea in order to reduce this uncertainty. In the context of our
560 study, this has several consequences:

- 561 • The average of the variables calculated for the eastern basin have a greater sensitivity
562 to outliers.
- 563 • The averages calculated at the Mediterranean Sea scale are necessarily closer to those
564 of the western basin. The eastern basin is therefore more likely to have significantly
565 different values from the Mediterranean Sea.

566 However, the results obtained in this study allow us to temper these potential limitations.
567 Indeed, the comparison of the basins showed that statistically significant variations are very

568 small (e.g. case of PP for the Tyrrhenian Sea). This is due, on the one hand, to a real chemical
569 homogeneity of the microplastic pollution of the Mediterranean Sea, which is reflected by
570 relatively close average values at the scale of the basins, and, on the other hand, to the difference
571 in the number of microplastics analysed for each of the basins in our calculations. Thus, the
572 lower number of microplastics analysed in the eastern basin results, on the one hand, in a greater
573 interval of confidence than for the other basins studied, and on the other hand, in statistical tests
574 that are less sensitive to the variations measured. This implies that by increasing the research
575 effort in this part of the Mediterranean Sea, the uncertainty could be sufficiently reduced to
576 show a significant difference between the western and eastern part of the Mediterranean Sea.

577 Finally, it is interesting to rely on proportion tests to compare the percentage of the different
578 chemical nature presented in previously published articles. Indeed, this type of test uses the
579 proportion and the number of particles analysed as input data to determine whether these values
580 are statistically different or not. This approach allows for an effective comparison of the results
581 obtained between two studies while taking into account the variability in analytical effort that
582 may exist between publications. The results will show whether there is a statistical difference
583 between the proportions. In the case of a significant difference, however, the test will not, be
584 able to determine whether this is related to a difference in protocol (apart from the number of
585 particles analysed, which is considered in the test) or to a real difference in terms of plastic
586 pollution. However, the use of this type of test implies that the input data (proportion and
587 number of microplastics analysed) are included in the publications, which is unfortunately not
588 always the case.

589 5. Conclusion

590 The objective of this work was to evaluate the chemical nature of the microplastic pollution at
591 the surface of the Mediterranean Sea sampled by Manta net during the Tara Mediterranean
592 expedition undertaken during the warm season (June-November) 2014.

593 Microplastic from 54 sites was analyzed by FTIR spectroscopy and size, concentrations in mass
594 and in number were measured. The main polymers identified in this work were PE 67,3+/-2,4%;
595 PP 20,8+/-2,1% and PS 3+/-0,9%. The results point towards a certain homogeneity of the
596 chemical nature of microplastics in the Mediterranean during the sampling period. However,
597 differences, confirmed by the literature, were observed at a mesoscale level. In particular, the
598 proportions of PE and PP were low in the North Tyrrhenian sea compared to the other subbasins.
599 However, new studies involving more targeted geographical or temporal sampling or numerical
600 modeling especially of the less explored areas such as the Alboran Sea, the Levantine Sea (both
601 offshore and nearshore) and the Adriatic Sea will confirm, invalidate or refine some of the
602 hypotheses made here.

603 ACKNOWLEDGMENTS

604 We thank the commitment of the following institutions, persons and sponsors: CNRS, UPMC,
605 LOV, Genoscope/CEA, the Tara Expeditions Foundation and its founders: agnès b.®, Etienne
606 Bourgois, Romain Troublé, the Veolia Environment Foundation, Lorient Agglomeration, Serge
607 Ferrari, the Foundation Prince Albert II de Monaco, IDEC, the “Tara” schooner and teams. We
608 thank MERCATOR-CORIOLIS and ACRI-ST for providing daily satellite data during the
609 expedition. We are also grateful to the French Ministry of Foreign Affairs for supporting the
610 expedition and to the countries that graciously granted sampling permission. We would like to
611 thank Marie Emmanuelle Kerros and Maryvonne Henry for their help in the analysis of plastics.
612 Finally, we thank Giuseppe Suaria for sharing his data with us.

613 REFERENCES

614 Andrady, A.L., 2017. The plastic in microplastics: A review. *Mar. Pollut. Bull.* 119, 12–22.
615 <https://doi.org/https://doi.org/10.1016/j.marpolbul.2017.01.082>

616 Andrady, A.L., 2011. Microplastics in the marine environment. *Mar. Pollut. Bull.* 62, 1596–
617 1605. <https://doi.org/10.1016/j.marpolbul.2011.05.030>

618 Avio, C.G., Gorbi, S., Regoli, F., 2017. Plastics and microplastics in the oceans: From emerging
619 pollutants to emerged threat. *Mar. Environ. Res.* 128, 2–11.
620 <https://doi.org/https://doi.org/10.1016/j.marenvres.2016.05.012>

621 Baini, M., Fossi, M.C., Galli, M., Caliani, I., Campani, T., Finoia, M.G., Panti, C., 2018.
622 Abundance and characterization of microplastics in the coastal waters of Tuscany (Italy):
623 The application of the MSFD monitoring protocol in the Mediterranean Sea. *Mar. Pollut.*
624 *Bull.* 133, 543–552. <https://doi.org/https://doi.org/10.1016/j.marpolbul.2018.06.016>

625 Bryant, J.A., Clemente, T.M., Viviani, D.A., Fong, A.A., Thomas, K.A., Kemp, P., Karl, D.M.,
626 White, A.E., DeLong, E.F., Jansson, J.K., 2016. Diversity and Activity of Communities
627 Inhabiting Plastic Debris in the North Pacific Gyre. *mSystems* 1, e00024-16.
628 <https://doi.org/10.1128/mSystems.00024-16>

629 Campanale, C., Stock, F., Massarelli, C., Kochleus, C., Bagnuolo, G., Reifferscheid, G.,
630 Uricchio, V.F., 2020. Microplastics and their possible sources: The example of Ofanto
631 river in southeast Italy. *Environ. Pollut.* 258, 113284.
632 <https://doi.org/https://doi.org/10.1016/j.envpol.2019.113284>

633 Chen, Xi, Xu, M., Yuan, L., Huang, G., Chen, Xiaojing, Shi, W., 2021. Degradation degree
634 analysis of environmental microplastics by micro FT-IR imaging technology.
635 *Chemosphere* 274, 129779.
636 <https://doi.org/https://doi.org/10.1016/j.chemosphere.2021.129779>

637 Cincinelli, A., Martellini, T., Guerranti, C., Scopetani, C., Chelazzi, D., Giarrizzo, T., 2019. A
638 potpourri of microplastics in the sea surface and water column of the Mediterranean Sea.
639 *TrAC Trends Anal. Chem.* 110, 321–326.
640 <https://doi.org/https://doi.org/10.1016/j.trac.2018.10.026>

641 Constant, M., Ludwig, W., Kerhervé, P., Sola, J., Charrière, B., Sanchez-Vidal, A., Canals, M.,
642 Heussner, S., 2020. Microplastic fluxes in a large and a small Mediterranean river
643 catchments: The Têt and the Rhône, Northwestern Mediterranean Sea. *Sci. Total Environ.*
644 716, 136984. <https://doi.org/https://doi.org/10.1016/j.scitotenv.2020.136984>

645 Cózar, A., Martí, E., Duarte, C.M., García-de-Lomas, J., van Sebille, E., Ballatore, T.J.,
646 Eguíluz, V.M., González-Gordillo, J.I., Pedrotti, M.L., Echevarría, F., Troublè, R.,
647 Irigoien, X., 2017. The Arctic Ocean as a dead end for floating plastics in the North
648 Atlantic branch of the Thermohaline Circulation. *Sci. Adv.* 3.
649 <https://doi.org/10.1126/sciadv.1600582>

650 Cózar, A., Sanz-Martín, M., Martí, E., González-Gordillo, J.I., Ubeda, B., Gálvez, J.Á.,
651 Irigoien, X., Duarte, C.M., 2015. Plastic Accumulation in the Mediterranean Sea. *PLoS*
652 *One* 10, e0121762. <https://doi.org/10.1371/journal.pone.0121762>

653 de Haan, W.P., Sanchez-Vidal, A., Canals, M., 2019. Floating microplastics and aggregate
654 formation in the Western Mediterranean Sea. *Mar. Pollut. Bull.* 140, 523–535.
655 <https://doi.org/https://doi.org/10.1016/j.marpolbul.2019.01.053>

656 Djellouli-Tabet, Y., 2010. Common Scarcity, Diverse Responses in the Maghreb Region BT -
657 Water and Sustainability in Arid Regions: Bridging the Gap Between Physical and Social
658 Sciences, in: Schneier-Madanes, G., Courel, M.-F. (Eds.), . Springer Netherlands,
659 Dordrecht, pp. 87–102. https://doi.org/10.1007/978-90-481-2776-4_6

660 Enders, K., Lenz, R., Stedmon, C.A., Nielsen, T.G., 2015. Abundance, size and polymer

661 composition of marine microplastics $\geq 10\mu\text{m}$ in the Atlantic Ocean and their modelled
662 vertical distribution. *Mar. Pollut. Bull.* 100, 70–81.
663 <https://doi.org/https://doi.org/10.1016/j.marpolbul.2015.09.027>

664 Fytianos, G., Ioannidou, E., Thysiadou, A., Mitropoulos, A.C., Kyzas, G.Z., 2021.
665 Microplastics in Mediterranean Coastal Countries: A Recent Overview. *J. Mar. Sci. Eng.*
666 . <https://doi.org/10.3390/jmse9010098>

667 Gasperi, J., Dris, R., Bonin, T., Rocher, V., Tassin, B., 2014. Assessment of floating plastic
668 debris in surface water along the Seine River. *Environ. Pollut.* 195, 163–166.
669 <https://doi.org/10.1016/j.envpol.2014.09.001>

670 Gorsky, G., Ohman, M.D., Picheral, M., Gasparini, S., Stemmann, L., Romagnan, J.-B.,
671 Cawood, A., Pesant, S., García-Comas, C., Prejger, F., 2010. Digital zooplankton image
672 analysis using the ZooScan integrated system. *J. Plankton Res.* 32, 285–303.
673 <https://doi.org/10.1093/plankt/fbp124>

674 Grosjean, P., Picheral, M., Warembourg, C., Gorsky, G., 2004. Enumeration, measurement, and
675 identification of net zooplankton samples using the ZOOSCAN digital imaging system.
676 *ICES J. Mar. Sci.* 61, 518–525. <https://doi.org/10.1016/j.icesjms.2004.03.012>

677 Guerranti, C., Perra, G., Martellini, T., Giari, L., Cincinelli, A., 2020. Knowledge about
678 Microplastic in Mediterranean Tributary River Ecosystems: Lack of Data and Research
679 Needs on Such a Crucial Marine Pollution Source. *J. Mar. Sci. Eng.* 8, 216.
680 <https://doi.org/10.3390/jmse8030216>

681 Gündoğdu, S., Çevik, C., Ayat, B., Aydoğan, B., Karaca, S., 2018. How microplastics quantities
682 increase with flood events? An example from Mersin Bay NE Levantine coast of Turkey.
683 *Environ. Pollut.* 239, 342–350.
684 <https://doi.org/https://doi.org/10.1016/j.envpol.2018.04.042>

685 Imhof, H.K., Ivleva, N.P., Schmid, J., Niessner, R., Laforsch, C., 2013. Contamination of beach
686 sediments of a subalpine lake with microplastic particles. *Curr. Biol.* 23, R867–R868.

687 Jambeck, J.R., Geyer, R., Wilcox, C., Siegler, T.R., Perryman, M., Andrady, A., Narayan, R.,
688 Law, K.L., 2015. Marine pollution. Plastic waste inputs from land into the ocean. *Science*
689 (80-.). 347, 768–771. <https://doi.org/10.1126/science.1260352>

690 Julienne, F., Delorme, N., Lagarde, F., 2019. From macroplastics to microplastics: Role of
691 water in the fragmentation of polyethylene. *Chemosphere* 236, 124409.
692 <https://doi.org/https://doi.org/10.1016/j.chemosphere.2019.124409>

693 Kedzierski, M., Falcou-Préfol, M., Kerros, M.E., Henry, M., Pedrotti, M.L., Bruzaud, S., 2019a.
694 A machine learning algorithm for high throughput identification of FTIR spectra:
695 Application on microplastics collected in the Mediterranean Sea. *Chemosphere* 234, 242–
696 251. <https://doi.org/10.1016/j.chemosphere.2019.05.113>

697 Kedzierski, M., Le Tilly, V., César, G., Sire, O., Bruzaud, S., 2017. Efficient microplastics
698 extraction from sand. A cost effective methodology based on sodium iodide recycling.
699 *Mar. Pollut. Bull.* 115. <https://doi.org/10.1016/j.marpolbul.2016.12.002>

700 Kedzierski, M., Villain, J., Falcou-Préfol, M., Kerros, M.E., Henry, M., Pedrotti, M.L.,
701 Bruzaud, S., 2019b. Microplastics in Mediterranean Sea: A protocol to robustly assess
702 contamination characteristics. *PLoS One* 14, e0212088.
703 <https://doi.org/10.1371/journal.pone.0212088>

704 Khan, F.R., Shashoua, Y., Crawford, A., Drury, A., Sheppard, K., Stewart, K., Sculthorp, T.,
705 2020. ‘The Plastic Nile’: First Evidence of Microplastic Contamination in Fish from the
706 Nile River (Cairo, Egypt). *Toxics* 8, 22. <https://doi.org/10.3390/toxics8020022>

707 Lacerda, A.L. d. F., Rodrigues, L. dos S., van Sebille, E., Rodrigues, F.L., Ribeiro, L., Secchi,

708 E.R., Kessler, F., Proietti, M.C., 2019. Plastics in sea surface waters around the Antarctic
709 Peninsula. *Sci. Rep.* 9, 3977. <https://doi.org/10.1038/s41598-019-40311-4>

710 Lebreton, L.C.M., Greer, S.D., Borrero, J.C., 2012. Numerical modelling of floating debris in
711 the world's oceans. *Mar. Pollut. Bull.* 64, 653–661.
712 <https://doi.org/10.1016/j.marpolbul.2011.10.027>

713 Liland, K.H., 2015. 4S Peak Filling – baseline estimation by iterative mean suppression.
714 *MethodsX* 2, 135–140. <https://doi.org/10.1016/j.mex.2015.02.009>

715 Liubartseva, S., Coppini, G., Lecci, R., Clementi, E., 2018. Tracking plastics in the
716 Mediterranean: 2D Lagrangian model. *Mar. Pollut. Bull.* 129, 151–162.
717 <https://doi.org/https://doi.org/10.1016/j.marpolbul.2018.02.019>

718 Mani, T., Hauk, A., Walter, U., Burkhardt-Holm, P., 2015. Microplastics profile along the
719 Rhine River. *Sci. Rep.* 5, 17988. <https://doi.org/10.1038/srep17988>

720 Martellini, T., Guerranti, C., Scopetani, C., Ugolini, A., Chelazzi, D., Cincinelli, A., 2018. A
721 snapshot of microplastics in the coastal areas of the Mediterranean Sea. *TrAC - Trends*
722 *Anal. Chem.* 109, 173–179. <https://doi.org/10.1016/j.trac.2018.09.028>

723 Napper, I.E., Davies, B.F.R., Clifford, H., Elvin, S., Koldewey, H.J., Mayewski, P.A., Miner,
724 K.R., Potocki, M., Elmore, A.C., Gajurel, A.P., Thompson, R.C., 2020. Reaching New
725 Heights in Plastic Pollution—Preliminary Findings of Microplastics on Mount Everest.
726 *One Earth* 3, 621–630. <https://doi.org/https://doi.org/10.1016/j.oneear.2020.10.020>

727 Newcombe, R.G., 1998a. Interval Estimation for the Difference Between Independent
728 Proportions: Comparison of Eleven Methods. *Stat. Med.* 17, 873–890.

729 Newcombe, R.G., 1998b. Two-Sided Confidence Intervals for the Single Proportion:
730 Comparison of Seven Methods. *Stat. Med.* 17, 857–872.

731 Pedrotti, M.L., Petit, S., Elineau, A., Bruzaud, S., Crebassa, J.C., Dumontet, B., Marti, E.,
732 Gorsky, G., Cozar, A., 2016. Changes in the Floating Plastic Pollution of the
733 Mediterranean Sea in Relation to the Distance to Land. *PLoS One* 11, e0161581.
734 <https://doi.org/10.1371/journal.pone.0161581>

735 Ripley, B.D., 1996. *Pattern recognition and neural networks*. Cambridge University Press,
736 Cambridge ; New York.

737 Sighicelli, M., Pietrelli, L., Lecce, F., Iannilli, V., Falconieri, M., Coscia, L., Di Vito, S., Nuglio,
738 S., Zampetti, G., 2018. Microplastic pollution in the surface waters of Italian Subalpine
739 Lakes. *Environ. Pollut.* 236, 645–651.
740 <https://doi.org/https://doi.org/10.1016/j.envpol.2018.02.008>

741 Soto-Navarro, J., Jordá, G., Deudero, S., Alomar, C., Amores, Á., Compa, M., 2020. 3D
742 hotspots of marine litter in the Mediterranean: A modeling study. *Mar. Pollut. Bull.* 155,
743 111159. <https://doi.org/https://doi.org/10.1016/j.marpolbul.2020.111159>

744 Suaria, G., Avio, C.G., Mineo, A., Lattin, G.L., Magaldi, M.G., Belmonte, G., Moore, C.J.,
745 Regoli, F., Aliani, S., 2016. The Mediterranean Plastic Soup: synthetic polymers in
746 Mediterranean surface waters. *Sci Rep* 6, 37551. <https://doi.org/10.1038/srep37551>

747 The R Core Team, 2019. *R: A Language and Environment for Statistical Computing*.

748 Thiel, M., Luna-Jorquera, G., Álvarez-Varas, R., Gallardo, C., Hinojosa, I.A., Luna, N.,
749 Miranda-Urbina, D., Morales, N., Ory, N., Pacheco, A.S., Portflitt-Toro, M., Zavalaga, C.,
750 2018. Impacts of Marine Plastic Pollution From Continental Coasts to Subtropical
751 Gyres—Fish, Seabirds, and Other Vertebrates in the SE Pacific . *Front. Mar. Sci.* .

752 Van Cauwenberghe, L., Devriese, L., Galgani, F., Robbins, J., Janssen, C.R., 2015.
753 *Microplastics in sediments: A review of techniques, occurrence and effects*. *Mar. Environ.*

754 Res. 111, 5–17. <https://doi.org/10.1016/j.marenvres.2015.06.007>

755 Varis, O., Taka, M., Kummu, M., 2019. The Planet’s Stressed River Basins: Too Much Pressure
756 or Too Little Adaptive Capacity? *Earth’s Futur.* 7, 1118–1135.
757 <https://doi.org/https://doi.org/10.1029/2019EF001239>

758 Veerasingam, S., Mugilarasan, M., Venkatachalapathy, R., Vethamony, P., 2016. Influence of
759 2015 flood on the distribution and occurrence of microplastic pellets along the Chennai
760 coast, India. *Mar. Pollut. Bull.* 109, 196–204.
761 <https://doi.org/https://doi.org/10.1016/j.marpolbul.2016.05.082>

762 Venables, W.N., Ripley, B.D., Venables, W.N., 2002. *Modern applied statistics with S*, 4th ed,
763 *Statistics and computing*. Springer, New York.

764 Vianello, A., Da Ros, L., Boldrin, A., Marceta, T., Moschino, V., 2018. First evaluation of
765 floating microplastics in the Northwestern Adriatic Sea. *Environ. Sci. Pollut. Res.* 25,
766 28546–28561. <https://doi.org/10.1007/s11356-018-2812-6>

767 Wakkaf, T., El Zrelli, R., Kedzierski, M., Balti, R., Shaiek, M., Mansour, L., Tlig-Zouari, S.,
768 Bruzard, S., Rabaoui, L., 2020. Characterization of microplastics in the surface waters of
769 an urban lagoon (Bizerte lagoon, Southern Mediterranean Sea): Composition, density,
770 distribution, and influence of environmental factors. *Mar. Pollut. Bull.* 160.
771 <https://doi.org/10.1016/j.marpolbul.2020.111625>

772 Wu, P., Tang, Y., Dang, M., Wang, S., Jin, H., Liu, Y., Jing, H., Zheng, C., Yi, S., Cai, Z.,
773 2020. Spatial-temporal distribution of microplastics in surface water and sediments of
774 Maozhou River within Guangdong-Hong Kong-Macao Greater Bay Area. *Sci. Total*
775 *Environ.* 717, 135187. <https://doi.org/https://doi.org/10.1016/j.scitotenv.2019.135187>

776 Yan, M., Nie, H., Xu, K., He, Y., Hu, Y., Huang, Y., Wang, J., 2019. Microplastic abundance,

777 distribution and composition in the Pearl River along Guangzhou city and Pearl River
778 estuary, China. *Chemosphere* 217, 879–886.
779 <https://doi.org/https://doi.org/10.1016/j.chemosphere.2018.11.093>

780 Zayan, A., Sayadi, S., Chevalier, C., Boukthir, M., Ben Ismail, S., Tedetti, M., 2020.
781 Microplastics in surface waters of the Gulf of Gabes, southern Mediterranean Sea:
782 Distribution, composition and influence of hydrodynamics. *Estuar. Coast. Shelf Sci.* 242,
783 106832. <https://doi.org/https://doi.org/10.1016/j.ecss.2020.106832>

784 Zeri, C., Adamopoulou, A., Bojanić Varezić, D., Fortibuoni, T., Kovač Viršek, M., Kržan, A.,
785 Mandić, M., Mazziotti, C., Palatinus, A., Peterlin, M., Prvan, M., Ronchi, F., Siljic, J.,
786 Tutman, P., Vlachogianni, T., 2018. Floating plastics in Adriatic waters (Mediterranean
787 Sea): From the macro- to the micro-scale. *Mar. Pollut. Bull.* 136, 341–350.
788 <https://doi.org/https://doi.org/10.1016/j.marpolbul.2018.09.016>

789 Zhang, K., Hamidian, A.H., Tubić, A., Zhang, Y., Fang, J.K.H., Wu, C., Lam, P.K.S., 2021.
790 Understanding plastic degradation and microplastic formation in the environment: A
791 review. *Environ. Pollut.* 274, 116554.
792 <https://doi.org/https://doi.org/10.1016/j.envpol.2021.116554>

793 Zhang, L., Liu, J., Xie, Y., Zhong, S., Gao, P., 2021. Occurrence and removal of microplastics
794 from wastewater treatment plants in a typical tourist city in China. *J. Clean. Prod.* 291,
795 125968. <https://doi.org/https://doi.org/10.1016/j.jclepro.2021.125968>

796

797